Numeric study of flow separation and shock reflection hysteresis in planar nozzles

Eilon Shimshi, Gabi Ben-Dor and Avi Levy
Pearlstone Center for Aeronautical Engineering Studies, Department of
Mechanical Engineering, Ben-Gurion University of the Negev, Beer Sheva, Israel

Abstract

A numerical study of the flow in overexpanded planar nozzles shows the existence of Mach reflection hysteresis inside an ideal nozzle while in tapered (constant angle) nozzles it does not appear. When including the geometry of the nozzle in the simulation it becomes evident that flow separation will occur before the transition from regular to Mach reflection for all relevant Mach numbers. The simulation reveals complex changes in the flow structure as the pressure ratio between the ambient and the stagnation is increased and decreased. Detailed examination of the pressure in the region of flow separation reveals an interaction between the shock cell structure and the location of the separation point. The pressure along the nozzle wall downstream of the separation point was found to be less than the ambient pressure with the affect being more pronounced in the case of the ideal nozzle. The formation of closed circulation bubbles may generate reverse flow separation.

1. INTRODUCTION

In planar overexpanded nozzle flows, a supersonic jet issuing from the nozzle outlet negotiates the pressure difference between the jet static pressure and the ambient conditions by creating an oblique shock that starts at the nozzle lip and is directed towards the symmetry plane. This incident shock (*IS*) can reflect either as a regular reflection (*RR*) or as a Mach reflection (*MR*) depending on the Mach number, ratio of specific heats and the pressure ratio between stagnation conditions in the inlet and the ambient pressure, termed *NPR*. By decreasing the *NPR* from fully expanded flow the angle of the *IS* is changed until at some *NPR* the *RR* transforms into an *MR*. The flow structure from an overexpanded nozzle is similar to the case of supersonic flow between wedges in which the type of reflection is dictated by the wedge angle (figure 1).
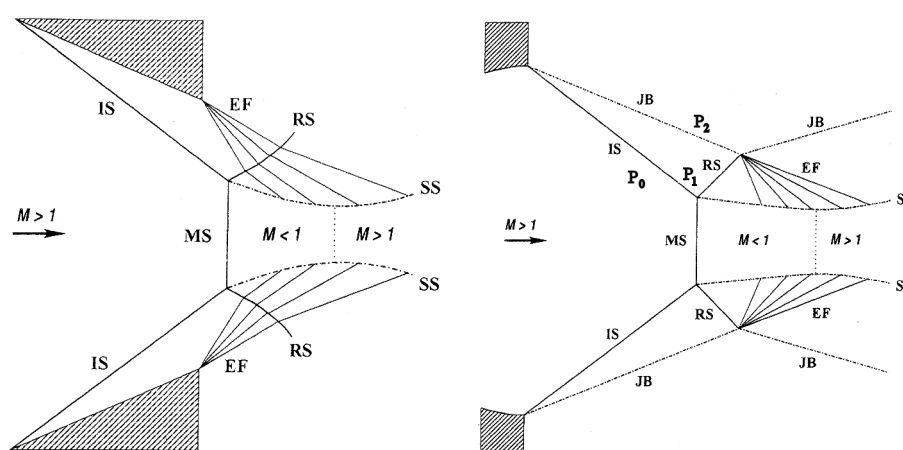

Figure 1. Similarity in flow structure between wedge flow (left) and nozzle flow (right). *IS*-incident shock, *RS*-reflected shock, *MS*-Mach stem, *JB*-jet boundary, *EF*- expansion fan, *SS*-slipstream [7]

Shock reflection hysteresis in the flow between wedges has been studied theoretically [1, 2], numerically [3] and experimentally [4, 5] during the past couple of decades. The possibility of such a phenomenon was first suggested by Hornung et al. [6] and was based on the occurrence of a dual-solution domain in the two-shock and three-shock theories developed by von Neumann in the mid 40's. Experimental verification was first provided by Chpoun et al. [4] in a wind-tunnel experiment.

The occurrence of this phenomenon in the outlet of an overexpanded converging diverging nozzle has only a few numerical references [7, 8]. To the best of our knowledge, no experimental work has been done on this subject.

It should be noted that although the flow pattern from an overexpanded axisymmetric jet appears to be very similar to the flow from a planer nozzle, there is a distinct difference between them. In the case of axisymmetric flows, a regular reflection is impossible [9-11] and thus no hysteresis can occur.

Reduced *NPR* is known to promote nozzle flow separation, this phenomenon is well known in rocket engine start-up transient and in operation of space vehicle rockets at sea level conditions. The condition for boundary layer separation in compressible flow can be expressed as [12]

$$\left. \frac{\partial \left(\rho u^2 \right)}{\partial y} \right|_{y=0} = 0$$

When the dynamic pressure is reduced to zero at the wall because of increasing pressure gradient in the direction of the flow the boundary layer will separate from the wall and reverse flow will occur.

1.1 Nozzle flow separation

Nozzle flow separation has been studied extensively over the past 50 years [13-16] because of its importance to rocket engine performance. There are several models (empirical and analytical) to predict the onset of flow separation as a function of pressure ratio. Frey [17] has an extensive review of flow separation models with comparisons to experimental results that show that in the Mach number range of 2.5-4.5 the agreement is good. Most of the empirical predictions are for axisymmetric nozzles and the ones that are for planar nozzles are mainly for tapered (constant angle) configuration [18]. It is still possible to use the predictions developed for axisymmetric nozzles for planar ones because in both cases separation at the wall is primarily driven by the balance between the momentum of the supersonic jet and static back pressure. Thus, for different Mach numbers, separation will initiate at different stagnation to ambient pressure ratios. Plotting the critical pressure ratio, which initiates separation as a function of Mach number from several models, shows that for all Mach numbers greater than about 2.2 flow separation will occur below the dual-solution domain (figure 2). This means that as pressure ratio increases from perfectly expanded to overexpanded conditions, flow separation will initiate before the transition from *RR* to *MR*. As the pressure ratio increases, the separation point will move upstream along the nozzle wall and thus the whole shock system will move back into the nozzle, but the general flow structure will remain the same.

This result precludes the possibility of a shock reflection hysteresis in the outlet of a planar nozzle because at Mach numbers below 2.2 the dual-solution domain reduces to null.

Even after flow separation occurs the flow pattern of an *RR* followed by an interaction between the jet boundary and the reflected shock does not change when the flow starts to separate from the nozzle wall. The flow pattern shifts upstream but the Mach number at the reflection point on the symmetry plane remains constant due to the fact that region downstream of the left running characteristic from the symmetry plane to the nozzle outlet is a uniform region. As the pressure ratio increases the oblique shock moves upstream and becomes steeper and the Mach number downstream of the *RR* approaches sonic conditions. The fact that the flow separation does not affect the reflection at the symmetry plane suggests that a transition from *RR* to *MR* is still possible at some pressure ratio.

1.2 Planar supersonic nozzles

Nozzles for propelling aircrafts or rockets are usually axisymmetric and come in a variety of configurations such as parabolic, truncated ideal contour (TIC), thrust optimized. Planar nozzles have fewer avionic applications and are more often found in testing facilities, they have two typical configurations, one is the ideal contour and the other is the tapered (wedge shape, constant angle) nozzle.
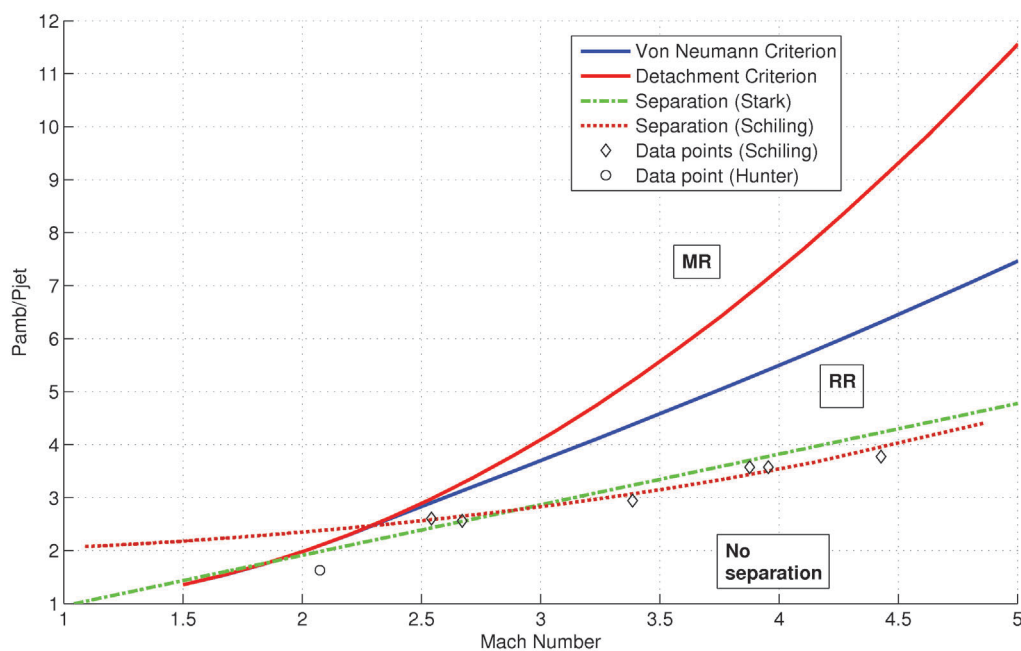
Figure 2. Pressure ratio criteria as a function of Mach number. Dashed lines - flow separation criteria (2 models), Solid lines - von-Neumann criterion for *MR* and detachment criterion for *RR, Markers - Experimental Data.*

In order to produce a uniform and parallel flow at a desired Mach number in the outlet of a converging diverging nozzle, a specific nozzle contour is required. Such a contour may be calculated by the method of characteristics (MoC). Sivells [19] nozzle design code for wind tunnels is a very comprehensive program that uses several techniques in order to compute a nozzle contour, which will produce the desired jet, taking into account the curvature of the sonic line at the throat, the centerline distribution of Mach numbers and the boundary layer growth along the wall. With the aid of this code, an ideal planar nozzle contour was constructed with the following characteristics:

Exit-to-throat area ratio $AR = 8$
Throat radius of curvature ratio $r_c = 16$
Exit Mach number $M_0 = 3.67$
Fluid properties of air $\gamma = 1.4$
No radial flow region
No boundary layer correction

The resulting contour was used to build the computational domain. The inviscid CFD computation shows excellent agreement with the MoC calculations (Figure 3a).

The tapered nozzle has a simple structure; the converging part is circular with the same radius of curvature as the ideal contour and the diverging section is a straight line at 10°. The joining of the circular and linear parts creates a discontinuity in the second derivative of the wall that produces expansion and compression waves inside the nozzle. The Mach number at the nozzle outlet is 3.67 as in the ideal nozzle but the flow field is not uniform. The flow is parallel at the symmetry plane but diverges linearly as the distance from the symmetry plane grows and becomes parallel to the wall in its vicinity. Inviscid simulation shows that the Mach number along the symmetry plane and the wall are almost identical apart from slight deviations that are the result of expansion and compression wave (Figure 3b).

When viscous terms were included in the numeric simulation, extensive flow separation was observed. From the point of separation on the wall, the incident shock propagated towards the symmetry plane and reflected as an *RR*, this phenomenon was observed in both nozzle configurations.

Flow separation in overexpanded supersonic nozzles depends on the balance between the momentum of the flow in the boundary layer and the static pressure it encounters.
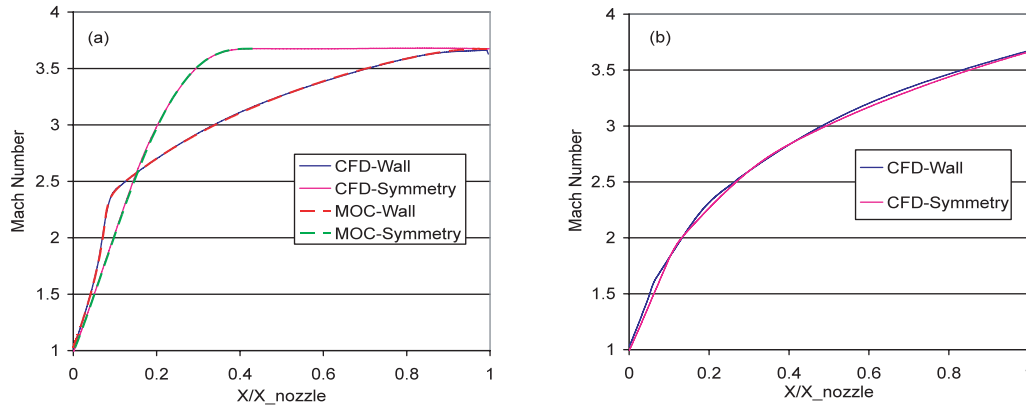
Figure 3. Mach number along nozzle wall and symmetry plane; (a) Ideal nozzle, (b) Tapered nozzle

The momentum can be expressed as ρu^2 (dynamic pressure). In the expanding part of a converging-diverging nozzle the flow accelerates but the density decreases so it is unclear whether the momentum increases or decreases. If we consider the case of quasi-one dimensional flow we can develop an expression for momentum normalized by the throat conditions

$$\frac{\rho u^2}{\left(\rho u^2\right)^*} = \frac{\rho}{\rho^*}\frac{u^2}{a^{*2}}\frac{a^2}{a^2} = M^2 \frac{\rho}{\rho^*}\frac{T}{T^*} \tag{1}$$

From isentropic relations for quasi-one dimensional flow

$$\frac{\rho_0}{\rho} = \left(1+\left(\frac{\gamma-1}{2}\right)M^2\right)^{\frac{1}{\gamma-1}} \tag{2}$$

$$\frac{\rho^*}{\rho_0} = \left(\frac{2}{\gamma+1}\right)^{\frac{1}{\gamma-1}} \tag{3}$$

Combining (2) and (3) results in:

$$\frac{\rho^*}{\rho} = \left(\frac{2}{\gamma+1}+\frac{\gamma-1}{\gamma+1}M^2\right)^{\frac{1}{\gamma-1}} \tag{4}$$

Similarly

$$\frac{T^*}{T} = \left(\frac{2}{\gamma+1}+\frac{\gamma-1}{\gamma+1}M^2\right) \tag{5}$$

Substituting equations (4) and (5) into equation (1) yields:

$$\frac{\rho u^2}{\left(\rho u^2\right)^*} = M^2 \left(\frac{2}{\gamma+1}+\frac{\gamma-1}{\gamma+1}M^2\right)^{\frac{-\gamma}{\gamma-1}} \tag{6}$$

Plotting this relation (figure 4a) for subsonic to supersonic Mach numbers $\gamma = 1.4$ we get a maximal momentum at $M = \sqrt{2}$ and at higher Mach numbers the momentum decreases, thus the likelihood of flow separation increases as the nozzle exit Mach number increases.

When the two nozzles are compared (figure 4b), the difference in the rate of expansion in them is manifested in the difference in momentum; at the outlet they are the same but towards the throat the tapered nozzle has a higher momentum. So it is expected that flow separation will start at the same *NPR* but as the stagnation pressure decreases its progression upstream will be earlier in the Ideal nozzle.
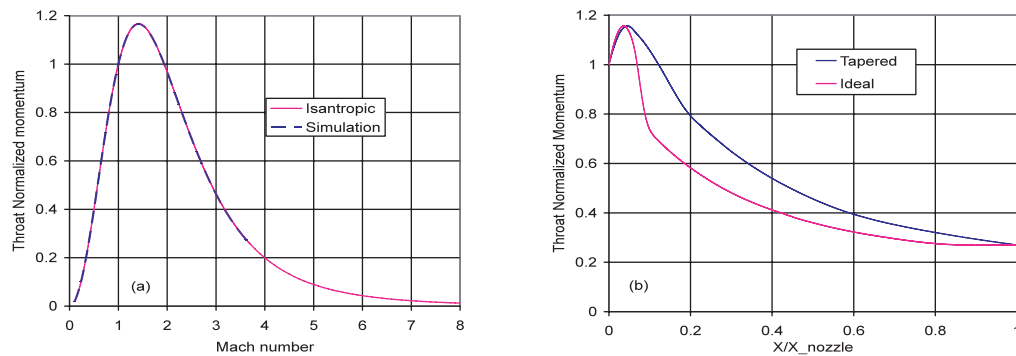
Figure 4. Flow momentum in a CD nozzle; (a) Comparison of CFD simulation and isentropic calculation, (b) momentum near the wall of ideal and tapered nozzles

2. NUMERIC METHOD

Numerical simulation of flow separation in turbulent supersonic flow regime is a challenging task. The standard k-ε turbulence model is inadequate in predicting the separation point because of the adverse pressure gradients at the wall as well as the compressibility effect of the supersonic flow. In a previous work [20] three variants of the two-equation model that are more suitable for such a flow were considered: the Realizable model, the Renormalization Group method k-ε model and the Shear-Stress-Transport (SST) k-ω model [21-23]. All three models gave similar results but the RNG k-ε method had better numerical behavior than the others.

The steady state Reynolds-averaged Navier-Stokes equations were solved using the commercial finite volume CFD program "FLUENT" using a 2D density based implicit solver, with a second order upwind discretization scheme. The computational domain was constructed with quadrilateral cells with special attention to the boundary layer and varying cell area according to the zones of interest. The nozzle zone was meshed densely while the jet outside the nozzle and the ambient zone above it were gradually coarsened as the distance downstream and away from the symmetry line increased. Early simulations showed that supersonic jets creates a suction effect, which draws fluid from the top and the right boundaries of the domain, and thus the boundary condition was set to "pressure inlet" instead of "pressure outlet". In order to reduce the number of elements in the domain a symmetry boundary condition was imposed and only the top part of the nozzle was modeled.

The simulation procedure was carried out in the following order. First, the pressure conditions at the inlet and outlet were set to produce overexpanded flow without separation. The calculation was iterated until the residuals flattened and the mass balance was within a 2% error margin. The stagnation pressure at the inlet was decreased by fixed pressure steps until the reflection changed to *MR*. Then the pressure was increased at the same increments until returning to the start conditions. The calculation was repeated with finer pressure steps around the pressure ratio of the *MR*↔*RR* transition. During the whole simulation, the pressure at the outlet of the nozzle was kept constant at 100 kPa.

A grid convergence study was performed by using three mesh densities and observing the effect on the resulting flow pattern.

All grid densities gave essentially similar results except for the region of discontinuity where the finer grids gave sharper changes in properties. The transition between *RR* and *MR* in the coarse grid was at a lower pressure ratio than in the medium grid, but the change when using the fine grid was minimal. It was therefore decided to use the medium grid density for the rest of the simulation.

It is well known that at low to moderate Mach numbers, flow separation in an overexapnded nozzle can be neither steady nor symmetric especially at low *NPRs* [24, 25], however the information about flow separation at higher Mach numbers is not as conclusive. In this numeric simulation it is assumed that flow separation is symmetric and steady.

3. RESULTS AND DISCUSSION

3.1 Ideal Nozzle

3.1.1 Flow structure on pressure decrease

Phase I - For 50>*NPR*>20 (figure 5a) a typical *RR* flow structure was formed consisting of a straight incident shock wave starting at the separation point and reflecting at the symmetry plane outside the

nozzle. Downstream of the reflected shock wave the flow is again parallel to the symmetry plane, while at the point the reflected shock hits the jet boundary a centered expansion fan is formed and the jet boundary is bent away from the symmetry plane. The reflection of the expansion fan from the symmetry plane and then from the jet boundary curves it again to form a dissipating repeating wavy structure (shock cells) whose wavelength depends on the *NPR*. As the *NPR* decreases, the reflection point moves upstream.

Phase II - For 20>*NPR*>11.8 (figure 5b) the point of separation shifts upstream to the extent that the reflection point is inside the nozzle. The incident shock wave is straight only downstream to the point where the last left running characteristic crosses the shock front, above this point the shock is bent because of the decreasing Mach number. A subsonic pocket develops downstream of the reflected shock wave between the first and second shock cells. As the stagnation pressure decreases, the subsonic pocket expands until it reaches the reflection point. The pressure downstream of the incident shock and above the jet boundary is lower than the ambient pressure, thus an upstream flow takes place and a recirculation zone develops (termed separation bubble). In the region between the jet and the wall, the total pressure starts to drop off at the nozzle exit plane and reaches its minimum value at the center of the separation bubble, which is located above the point where the jet boundary starts curving upwards.
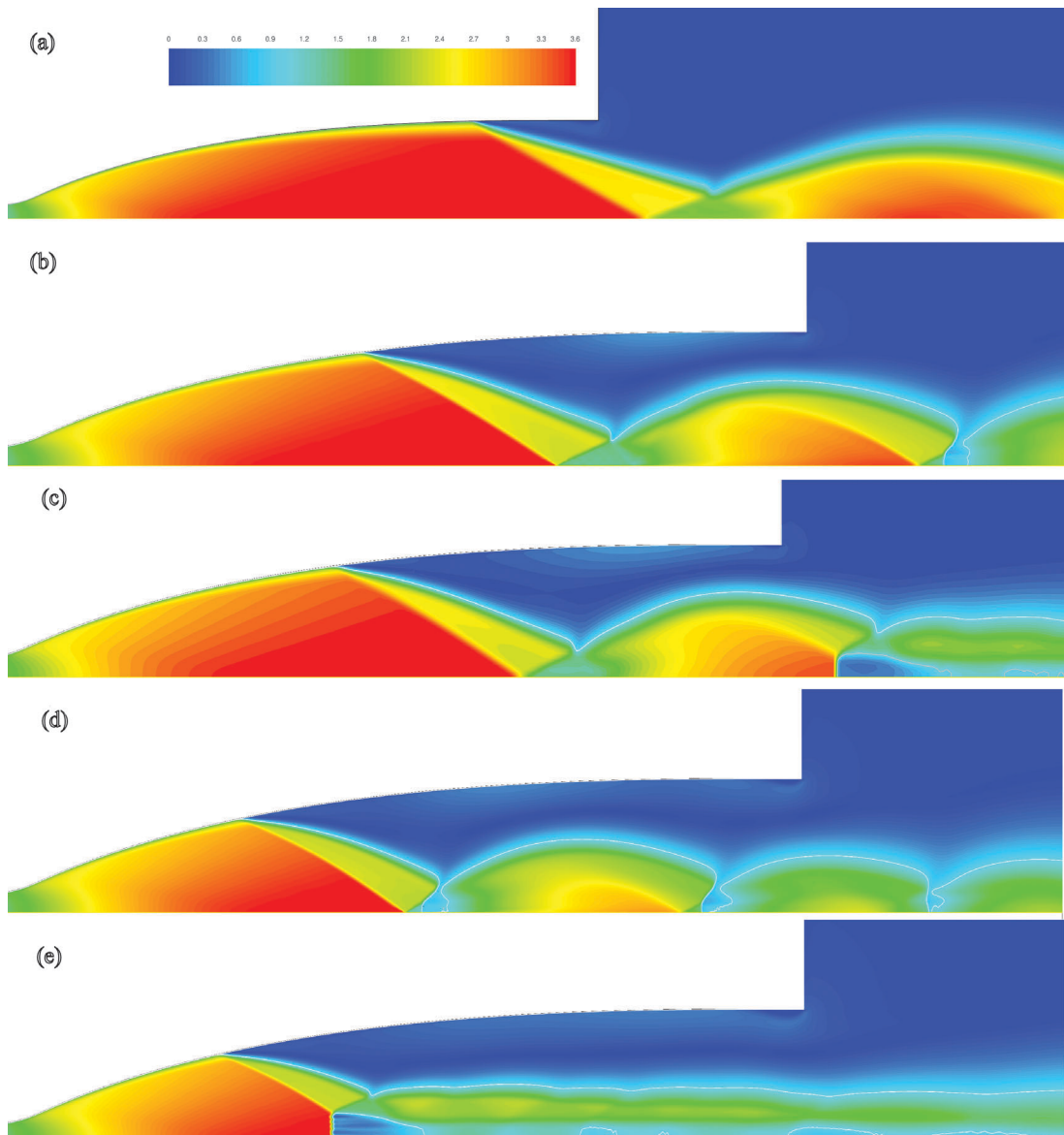

Figure 5. Mach contours in an ideal nozzle while reducing *NPR*; (a) *NPR*=25, (b) *NPR*=12.2, (c) *NPR*=10.2, (d) *NPR*=9.8, (e) *NPR*=9.3

Phase III - For 11.8>*NPR*>9.9 (figure 5c) the *RR* between the first and second shock cell abruptly transforms into an *MR*. Subsequent shock cells disappear and instead a straight jet with a subsonic inner jet core develops. As the pressure ratio increases, the Mach stem height diminishes as it moves upstream into the nozzle. The point of minimum total pressure in the recirculation zone moves upstream with the crest of the first shock cell.

Phase IV - For 9.9>*NPR*>9.4 (figure 5d), the *MR* between the first and second shock cell reverts back to *RR* and the shock cell structure downstream is reestablished. A subsonic pocket develops in the region downstream of the first *RS*, and as the pressure increases it expands towards the reflection point. A second separation bubble appears between the first and the second shock cells.

Phase V - For *NPR*<9.4 (figure 5e), the primary *RR* transforms into an *MR* and subsequent shock cells disappear. The *RR→MR* transition takes place when the subsonic pocket reaches the reflection point; this suggests that the transition takes place at the sonic criterion. As the pressure ratio decreases, the Mach stem becomes larger. The pressure in the separated area is more uniform and closer to the ambient value. The separation bubbles unite into a prolonged one.

3.1.2 Flow structure on pressure increase
Phase I - For *NPR*<13.4 (figure 6a), a typical *MR* flow structure persists. It consists of a nearly perpendicular Mach stem, and a triple point where the *IS, RS, MS* and the slipstream connect. The slipstream is parallel to the symmetry plane, which suggests that the reflection is close to the von-Neumann criterion. As the *NPR* is increased the Mach stem decreases in size and moves downstream, also the jet boundary, which is almost straight at first, becomes more and more wavy; accordingly the Mach number above and below the slipstream increases and a shock cell structure reemerges.

Phase II - For 13.4<*NPR*<14.2 (figure 6b), the primary *MR* disappears and the *RR* flow structure reappears. The reflection type between the first and second shock cells is an *MR* with the Mach stem getting smaller as the *NPR* is increased.

Phase III - For *NPR*>14.2, (figure 6c) the flow structure is identical to the one observed during the pressure increase phase I.
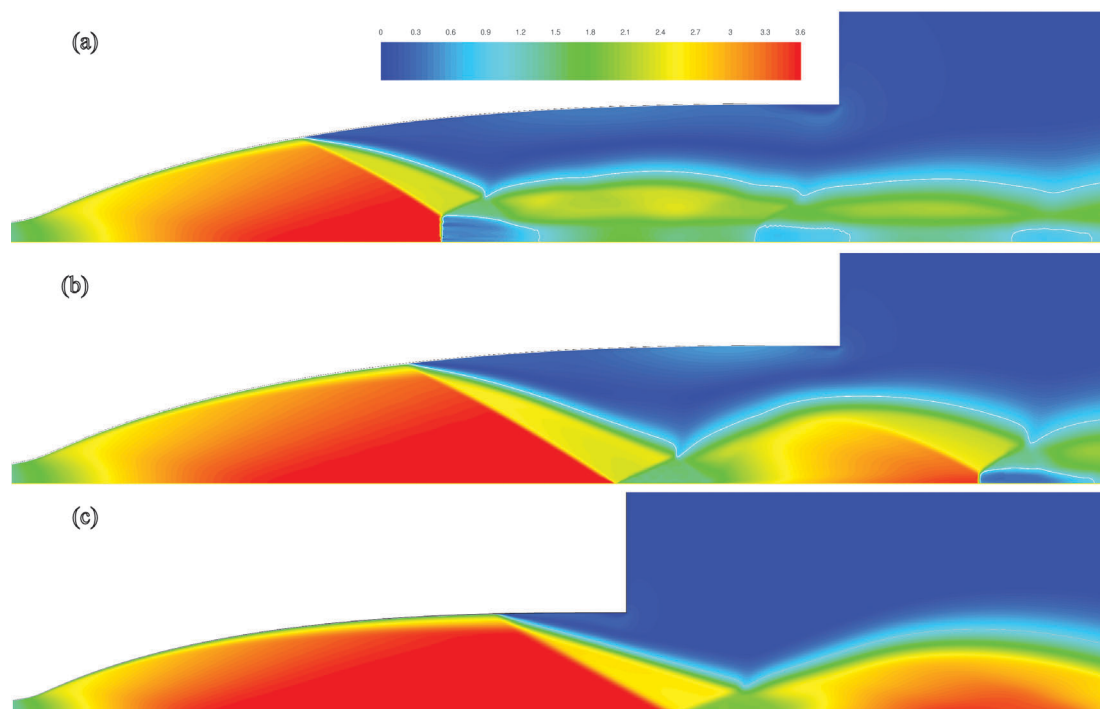

Figure 6. Mach contours in an ideal nozzle while increasing *NPR*; (a) *NPR*=11.4, (b) *NPR*=13.8, (c) *NPR*=25

3.2 Tapered Nozzle
3.2.3 Flow structure on pressure decrease

Phase I - For 34<*NPR*<22 (figure 7a) an *RR* flow structure is formed with the reflection point outside the nozzle. The separation point on the wall moves upstream as *NPR* is decreased. The Mach number just upstream of the separation point and the reflection point decreases steadily with *NPR*.

Phase II - For 22<*NPR*<10, (figure 7b) an *RR* is maintained with the point of reflection being inside the nozzle. The size of the shock cell is considerably larger than the cell size in the ideal nozzle for the same pressure ratio even though the Mach number is lower. There are no subsonic patches in the jet between the shock cells. The incident shock and the jet boundary from the separation point to the interaction with the reflected shock are straight although the flow conditions upstream aren't uniform.

Phase III - For 10<*NPR*<3.59, (figure 7c) the number of shock cells inside the nozzle increases as *NPR* decreases. Subsonic regions appear between the supersonic cells downstream of the incident shock. As NPR decreases the subsonic region in the first shock cell approaches the point of reflection.

Phase IV - For *NPR*<3.59, (figure 7d) the *RR* is transformed into an *MR* with a small Mach stem. As the pressure ratio decreases the Mach stem grows in size. The flow structure in the following shock cells remains practically unchanged. The slipstream downstream of the triple point is horizontal and the flow is subsonic both above and below it.
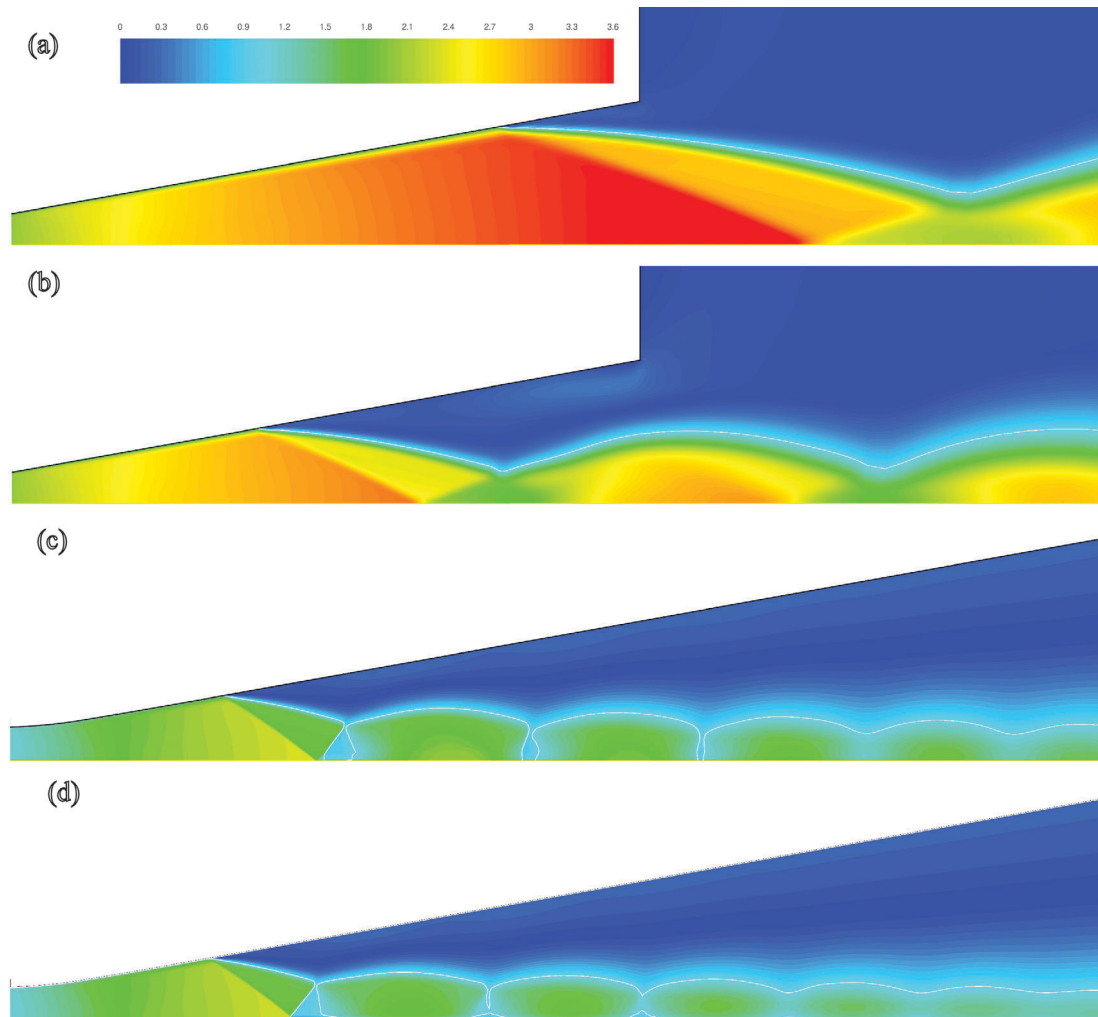

Figure 7. Mach contours in a tapered nozzle while increasing or reducing *NPR*; (a) *NPR*=27.6, (b) *NPR*=13.8, (c) *NPR*=3.7, (d) *NPR*=3.4

3.2.4 Flow structure on pressure increase
The flow structure is identical to the case of pressure ration decrease for the same *NPRs*, there is no hysteresis in this type of nozzle

3.3 Transition process
At low overexpansion the flow structure of both nozzles is similar, but at lower *NPRs* the difference is more pronounced because of the reducing Mach number in the tapered nozzle. In both nozzles the *IS* is relatively straight although the upstream Mach number is not constant. On the other hand the *JB* curvature depends on the uniformity of the flow conditions upstream of the *IS*. The shock angle in the ideal nozzle is larger than in the tapered nozzle for the same *NPR* and as a result the wave length of the shock cells is larger. The *RR→MR* transition takes place at *NPR*=9.4 for the ideal nozzle while at *NPR*=3.6 in the tapered nozzle.

Plotting the relation between Mach number and pressure ratio between the jet and the pressure in the separated area for each of the nozzles on the transition chart shown in figure 2 reveals the major difference between them. For the ideal nozzle one gets a vertical line crossing from the "no separation" region up to the separated *MR* region while for the tapered nozzle the line is almost horizontal and remains in the separated *RR* region most of process. When it crosses to the separated *MR* region it is in the area where the dual-solution domain is reduced almost to null (figure 8).
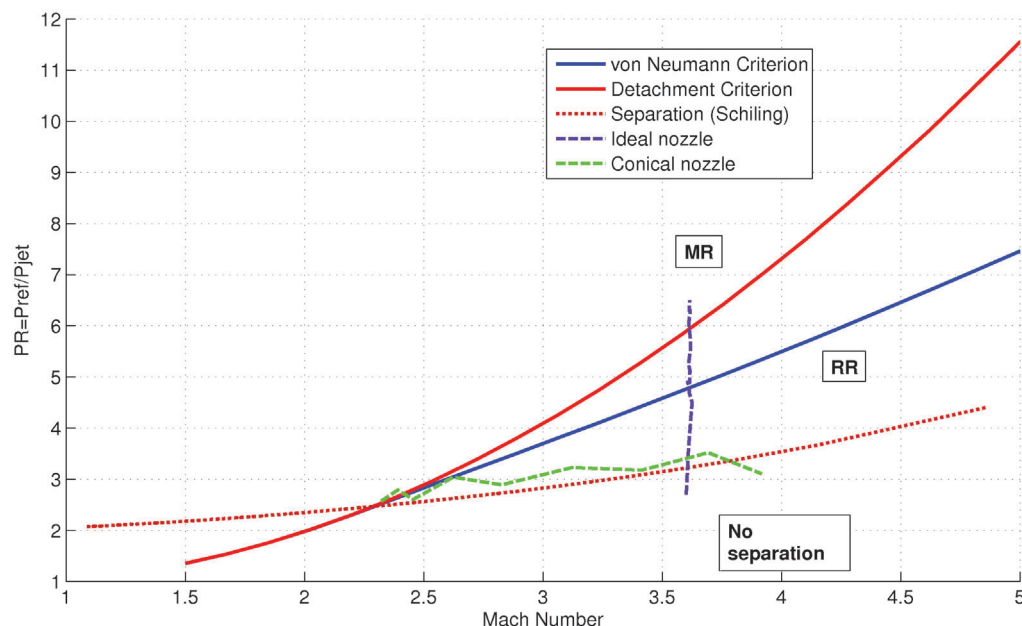

Figure 8: Flow separation regions showing the shock reflection [17] transition process of an ideal and tapered nozzle

3.4 Location of separation point
The location of the separation point depends on the balance between the momentum of the fluid in the boundary layer and the increasing pressure difference that it encounters. In the ideal nozzle the flow expands rapidly at first and then straightens out while in the tapered nozzle the expansion is constant, as a result the Mach number at the wall is greater for the ideal nozzle at the start of the diverging section, but tends to equalize towards the nozzle outlet. As a result the momentum is equal for both nozzles at the outlet but becomes smaller for the ideal nozzle as the separation point moves upstream. So it is expected that flow separation will start at the same *NPR* in both nozzles but as the stagnation pressure decreased its progression upstream will be earlier in the ideal nozzle. However, the simulation shows that in the ideal nozzle separation starts at a higher *NPR* than in the tapered nozzle (figure 9). This separation is minimal up till the pressure ratio that initiates flow separation in the tapered nozzle. This could be attributed to nozzle-exit effects as suggested by Morrisette & Goldberg [26]. At *NPR*<34

the rate of separation is higher in the ideal nozzle as expected from the momentum curve, but at *NPR*<20 this trend changes and the rate of separation slows down in the ideal nozzle. This change coincides with the entry of the crest of the first shock cell into the nozzle, this creates a close separation bubble and reduces the pressure in the separated area and reduces the pre-to-post separation pressure ratio. When the reflection type is changed from *RR* to *MR* the shock cell structure disappears and the separation pressure ratio increases again, accelerating the separation. In the tapered nozzle the rate of separation with decreasing *NPR* is more or less constant although the same mechanism exists, this may be due to the reducing Mach number at the symmetry plane. In the tapered nozzle the Mach number reduces with *NPR* reduction, this determines the size and waviness of the jet boundary (the envelope of the shock cells) and in turn increases the distance between the jet boundary and the wall of the nozzle, thus reducing the pressure loss due to the closed circulation bubbles. Figure 10a shows the wall pressure along the wall of the ideal nozzle from the point of separation for different *NPRs*, notice that at *NPR*>20 the pressure profile is self similar and close to the ambient pressure, but at *NPR*<20 the pressure along the wall decreases with *NPR*. This effect is smaller in the tapered nozzle (figure 10b) and starts at *NPR*<17.
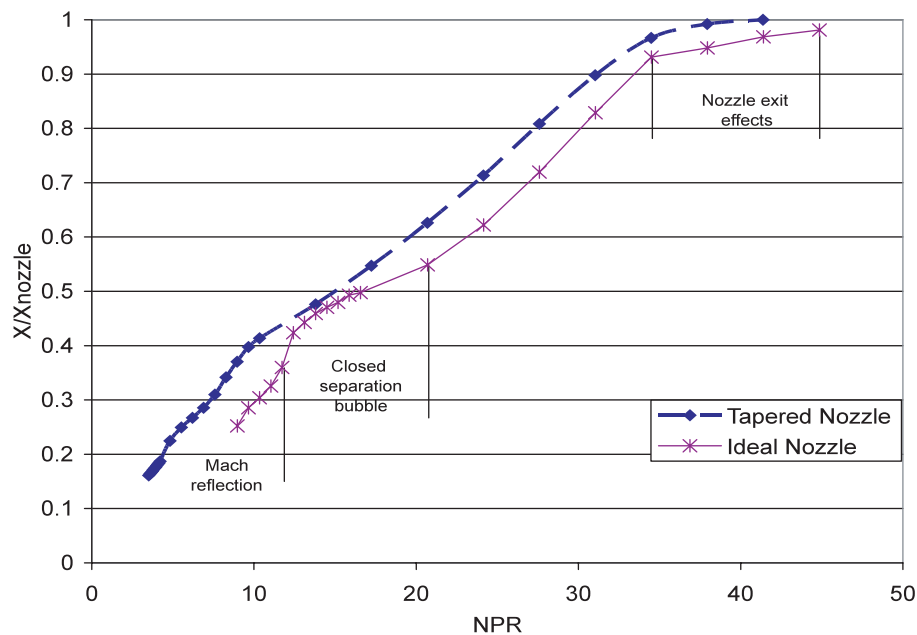

Figure 9. Location of separation point on the wall for ideal and tapered nozzles

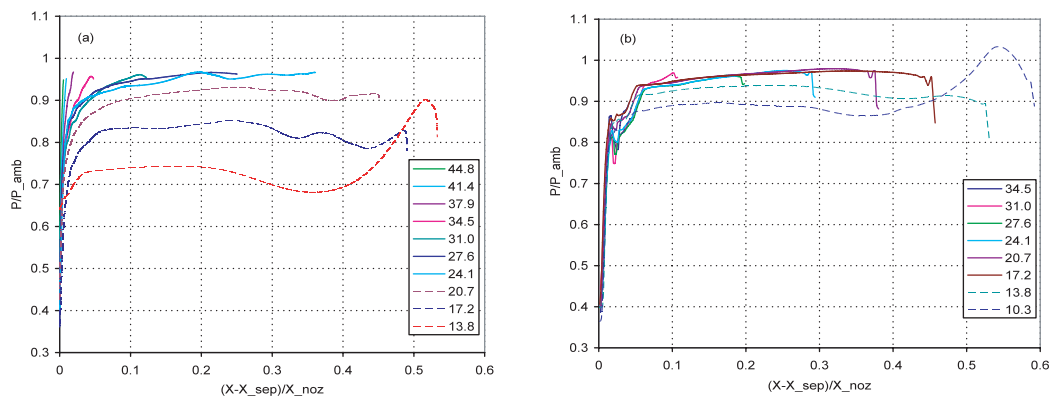
Figure 10: Pressure along the wall from the point of separation to the nozzle exit at different *NPRs*; (a) Ideal nozzle, (b) Tapered nozzle

3.5 Reverse flow separation

When flow separation starts, ambient fluid is sucked into the nozzle and flows along the wall of the nozzle in a reverse direction to the flow of the jet. As the shock cells move into the nozzle and form closed separation bubbles that reduce the pressure locally they create an adverse pressure gradient for the reverse flow along the nozzle wall. This causes flow separation of the reverse flow into the nozzle. The flow along the wall is downstream before the point of separation, then upstream and again downstream after the reverse flow separation. Figure 11 shows x-velocity vectors at NPR=17.2, the area of reverse separation correlates to the region in which the pressure rises in the negative x direction as seen at 0.23<x<0.38 of figure 10a.
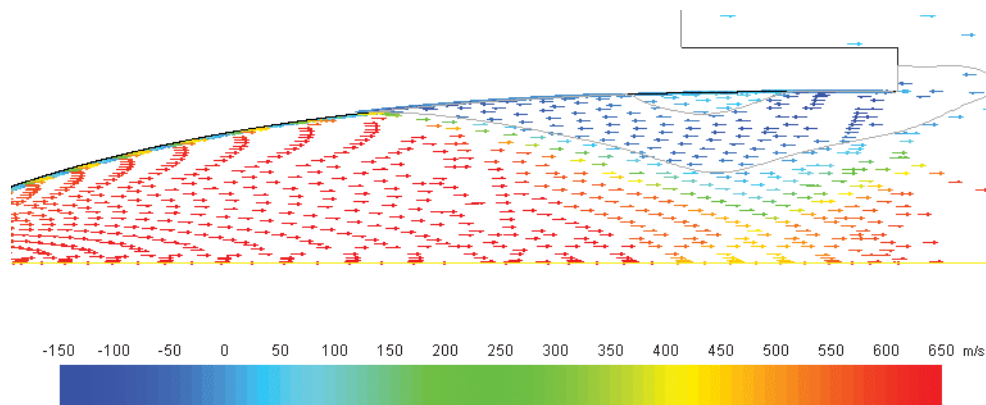

Figure 11. x-velocity vectors in an ideal nozzle showing a region of reverse flow separation at NPR=17.2; solid line-zero x-velocity

3.6 Location of the reflection point

The reflection point of the incident shock wave is affected by the Mach number upstream of the shock in the vicinity of the symmetry plane, the location of the separation point and the geometry of the nozzle and the pressure in the separated area. In the ideal nozzle the Mach number is constant along the symmetry plane while in the tapered nozzle it decreases as the separation move upstream. With all these factors affecting the reflection location, it is surprising to find a linear correlation between the location of the separation point and the reflection point for both nozzles (figure 12).
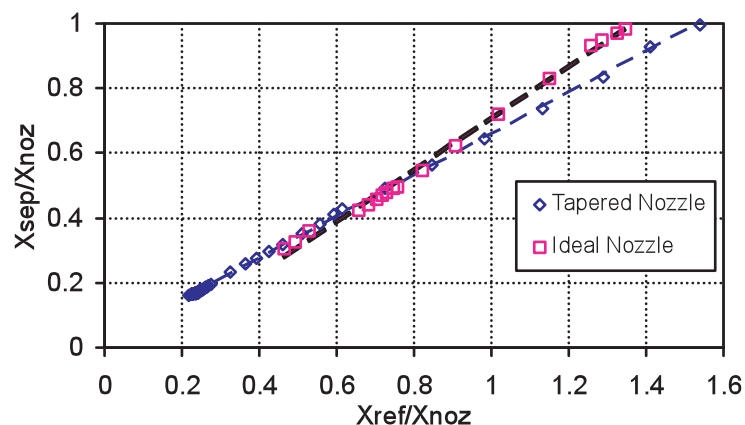

Figure 12: Relation between point of separation and point of reflection in ideal and tapered nozzles

At NPR>17 the reflection point is further downstream for the tapered nozzle, while at lower values it is similar for both.

4. CONCLUSION

A CFD computation using a two equations Navier-Stokes commercial solver was performed to simulate the flow in overexpanded nozzles at different *NPRs*. In planar overexpanded supersonic jets at high Mach numbers, transition form *RR* to *MR* cannot occur without flow separation. In ideal nozzles, shock reflection hysteresis can occur even though there is extensive flow separation. In tapered nozzles where the Mach number at the symmetry plane reduces as the point of reflection moves upstream with increasing flow separation it is unlikely that shock reflection hysteresis will be present. A strong interaction was found between the shock cell structure and the pressure in the separated region. The appearance of closed circulation bubbles reduces the local pressure compared to the ambient conditions and slows down the progression of separation. The locally reduced pressure may initiate a reverse flow separation.

1. REFERENCES

[1]   Li, H. and Ben-Dor, G., A parametric study of Mach reflection in steady flows, *Journal of Fluid Mechanics*, 341, 1997, pp. 101-125.

[2]   Schotz, M., Levy, A., Ben-Dor, G. and Igra, O., Analytical prediction of the wave configuration size in steady flow Mach reflections, *Shock Waves*, 7(6), 1997, pp. 363-72.

[3]   Vuillon, J., Zeitoun, D. and Ben-Dor, G., Reconsideration of oblique shock wave reflections in steady flows. Part 2. Numerical investigation, *Journal of Fluid Mechanics*, 301, 1995, pp. 37-50.

[4]   Chpoun, A., Passerel, D., Li, H. and Ben-Dor, G., Reconsideration of oblique shock wave reflections in steady flows. Part 1. Experimental investigation, *Journal of Fluid Mechanics*, 301, 1995, pp. 19-35.

[5]   Ivanov, M.S., Vandromme, D., Fomin, V.M., Kudryavtsev, A.N., Hadjadj, A. and Khotyanovsky, D.V., Transition between regular and Mach reflection of shock waves: New numerical and experimental results, *Shock Waves*, 11, 2001, pp. 99-107.

[6]   Hornung, H.G., Oertel, H. and Sandeman, R.J., Transition to Mach reflection of shock waves in steady and pseudosteady flow with and without relaxation, *Journal of Fluid Mechanics*, 90, 1979, pp. 541-60.

[7]   Hadjadj, A., Numerical investigation of shock reflection phenomena in overexpanded supersonic jets, *AIAA Journal*, 42(3), 2004, pp. 570-577.

[8]   Kudryavtsev, A.N., Khotyanovsky, D.V., Hadjadj, A., Vandromme, D. and Ivanov, M.S., Numerical investigation of shock wave interactions in supersonic imperfectly expanded jets, *International Conference on the Methods of Aerophysical Research*, (Vol. III), 2002, pp. 138-143.

[9]   Ralov, A.I., On the impossibility of regular reflection of a steady-state shock wave from the axis of symmetry, *Journal of Applied Mathematics and Mechanics*, 54(2), 1990, pp. 200-203.

[10]   Molder, S., Gulamhassein, A., Timofeev, E. and Voinovich, P., Focusing of conical shocks at the centre-line of symmetry, *21st International Symposium on Shock Waves*, Great Keppel Island, Australia, 1997, pp. Paper 5601.

[11]   Courant, R. and Friedrichs, K.O., *Supersonic flow and shock waves*, Interscience Publishers, New York, 1948, pp. 464.

[12]   Chang, P.K., *Control of flow separation: energy conservation, operational efficiency, and safety*, Hemisphere Pub. Co., Washington, 1976, pp. 523.

[13]   Summerfield, M., Foster, C.R. and Swan, W.C., Flow separation in overexpanded supersonic exhaust nozzles, *Jet Propulsion*, 24(9), 1954, pp. 319-321.

[14]   Reshotko, E., and Tucker, M., *Effect of a discontinuity on turbulent boundary-layer-thickness parameters with application to shock-induced separation*, NACA, TN 3454, 1955.

[15]   Romine, G.L.1., Nozzle flow separation, *AIAA Journal*, 36(9), 1998, pp. 1618-25.

[16]   Nasuti, F., Onofri, M. and Pietropaoli, E., The influence of nozzle shape on the shock structure in separated flows, *Proceedings of the 5th European Symposium on Aerothermodynamics for Space Vehicles*, 2004, pp. 353-358.

[17]   Frey, M., *Investigation of flow problems in rocket nozzles at overexpansion*, PhD Thesis, University of Stuttgart, 2001, 145p.

[18] Hunter, C.A., Experimental, theoretical, and computational investigation of separated nozzle flows, *34th AIAA/ASME/SAE/ASEE Joint Propulsion Conference & Exhibit*, AIAA, United States, 1998,

[19] Sivells, J.C., *A computer program for the aerodynamic design of axisymmetric and planar nozzles for supersonic and hypersonic wind tunnels*, Arnold Engineering Development Center, AEDC-TR-78-63, United States, 1978.

[20] Shimshi, E., Ben-Dor, G. and Levy, A., Viscous simulation of shock-reflection hysteresis in overexpanded planar nozzles, *Journal of Fluid Mechanics*, 635(-1), 2009, pp. 189-206.

[21] Menter, F.R., *Two-equation eddy-viscosity turbulence models for engineering applications*, AIAA Journal, 32(8), 1994, pp. 1598-1605.

[22] Mulvany, N.J., Chen, L., Tu, J.Y., *Steady-state evaluation of two-equation RANS (Reynolds-averaged Navier- Stokes) turbulence models for high-Reynolds number hydrodynamic flow simulations*, DSTO Platform Sciences Laboratory, DSTO-TR-1564, Australia, 2004.

[23] Speziale, C.G. and Thangam, S., Analysis of an RNG based turbulence model for separated flows, *International Journal of Engineering Science*, 30(10), 1992, pp. 1379-88.

[24] Reijasse, P., Corbel, B. and Soulevant, D., Unsteadiness and asymmetry of shock-induced separation in a planar two-dimensional nozzle: A flow description, *30th AIAA Fluid Dynamics Converence*, AIAA, 1999, pp. 1-10.

[25] Bourgoing, A. and Reijasse, P., Experimental analysis of unsteady separated flows in a supersonic planar nozzle, *Shock Waves*, 14(4), 2005, pp. 251-8.

[26] Morrisette, E.L., and Goldberg, T.J., *Turbulent-flow separation criteria for overexpanded supersonic nozzles*, NASA Langley Research Center, NASA-TP-1207, United States, 1978.